

Optical Properties and Chemical Compositions of Iodine-Containing Aerosols Produced from the Atmospheric Photolysis of Methylene Iodide in the Presence of Ozone

Yosuke Sakamoto,[1] Akihiro Yabushita,[1] Masahiro Kawasaki,*[1] Tomoki Nakayama,[2] and Yutaka Matsumi[2]

[1]Department of Molecular Engineering, Kyoto University, Kyoto 615-8510

[2]Solar-Terrestrial Environment Laboratory, Nagoya University, Nagoya 464-8601

Received February 3, 2009; E-mail: kawasaki@moleng.kyoto-u.ac.jp

Optical properties of iodine-containing aerosols that were produced by ultraviolet photoirradiation of a mixture gas of CH_2I_2 and O_3 with dry air diluent have been measured using a nephelometer, a particle soot absorption photometer and a cavity ring-down spectrometer. Single scattering albedo of iodine aerosols was determined to be 0.96 ± 0.01 at around 530 nm. Chemical compositions of the aerosols associated with particle size in the range of 0.2–1 μm was measured using a laser-ionization single-particle aerosol mass spectrometer. Positive and negative ion signals of iodine and iodine oxides, IO_n ($n = 0$–4), I_2O_n ($n = 0$–6), and I_3O_n ($n = 0$–1), carbon-containing compounds and HOI were detected.

The first detection of aerosol nucleation bursts at Mace Head, Ireland, was reported by O'Dowd et al.[1,2] and Grenfell et al.[3] Following the first detection, several studies of iodine-containing particle formation mechanisms have been performed.[4–11] Chemical compositions of iodine particle were measured by aerosol mass spectroscopy.[6] Hoffmann et al.[4] found the newly formed particles are purely composed of iodine oxides using CH_2I_2 as a precursor species. CH_2I_2 has been known to be a major photochemical source of iodine atoms in the marine boundary layer. They suggested that the multiple addition of OIO is a major step leading to particle formation. Burkholder et al.[7] reported a modeling study that very high concentrations of OIO have to be present to produce the particles.

$$CH_2I_2 + h\nu \rightarrow CH_2I + I \quad (1)$$

$$I + O_3 \rightarrow IO + O_2 \quad (2)$$

$$IO + IO \rightarrow OIO + I \quad (3)$$

$$OIO + OIO \rightarrow I_2O_4 \quad (4)$$

$$I_2O_4 + OIO \rightarrow\rightarrow\rightarrow \text{particle} \quad (5)$$

Iodine oxides are believed to form clusters based on studies of chemical compositions of iodine aerosols.[9–11] Formation of iodine oxides (IO and OIO) in the gas-phase has previously been confirmed in the photoreactions of CH_2I_2 with O_3.[12] Saunders and Plane,[11] who reported that fractal morphologies of iodine oxide nanoparticles generated photochemically from I_2 in the presence of O_3, are composed of I_2O_5 using transmission electron microscopy. They also performed quantum calculations showing that gas-phase I_2O_5 could be formed by a series of exothermic reactions.

$$IO + IO \xrightarrow{M} I_2O_2 \quad (6)$$

$$IO + OIO \xrightarrow{M} I_2O_3 \quad (7)$$

$$OIO + OIO \xrightarrow{M} I_2O_4 \quad (8)$$

$$I_2O_2 \xrightarrow{O_3} I_2O_3 \xrightarrow{O_3} I_2O_4 \xrightarrow{O_3} I_2O_5 \text{ (gas} \rightarrow \text{solid)} \rightarrow\rightarrow\rightarrow \text{particle} \quad (9)$$

Aerosol contributes to radiative forcing by scattering and absorption of incoming solar radiation and outgoing thermal radiation from the Earth's surface.[13] Since iodine and iodine oxides (e.g., I_2, IO, and OIO) have an absorption in the visible region, iodine aerosols may also have an absorption in the visible region.

In this study, chemical composition of iodine-containing particles has been measured by a laser-ionization single-particle aerosol mass spectrometer (LISPA-MS), and extinction, scattering and absorption coefficients by a nephelometer, a particle soot absorption photometer (PSAP) and a cavity ring-down spectrometer (CRDS).

Experimental

Preparation of Iodine-Containing Aerosols in a Teflon Bag. A mixture of CH_2I_2 and O_3 with synthetic air diluent was introduced into a Teflon bag (Tedler, 100 L) under atmospheric pressure. The bag was then continuously irradiated using a black lamp (Toshiba, peak wavelength at 352 nm, 20 W). Ozone was produced by irradiating an oxygen gas flow (760 Torr) with a low-pressure mercury pen-ray lamp (Hamamatsu Photonics, L937-02, 184.9 nm). The gas flow rates were controlled by mass flow controllers (STEC, SEC-E40) when gases were mixed into the bag. Ozone concentrations were measured upstream of the Teflon bag by monitoring the absorption at 253.7 nm ($\sigma = 1.15 \times 10^{-17}$ cm^2 $molecule^{-1}$ [14]) using a separate pen-ray lamp (Hamamatsu Photonics, L937-03) as a light source. All reagents were obtained from commercial sources. CH_2I_2 (Sigma-Aldrich, 99%), N_2 (>99.999%), synthetic air, and O_2 (>99.995%) were used without further purification. All experiments were conducted at room

Published on the web July 10, 2009; doi:10.1246/bcsj.82.910

temperature. The number size distribution of aerosol particles was monitored by optical particle counter (OPC, RION, KR-12A, diameter regions: 0.3–0.5, 0.5–0.7, 0.7–1.0, 1.0–2.0, 2.0–5.0, and >5.0 μm).

Analysis of Chemical Compositions of Iodine-Containing Aerosols. Chemical compositions of the iodine-containing aerosols were analyzed using LISPA-MS. The details of laboratory built LISPA-MS have been previously described.[15] Briefly, aerosol particles were focused into a particle beam by an aerodynamic lens.[16] After exiting the lens, the particle beam was transmitted into an ionization region. For detecting the particles introduced into the ionization region, a continuous-wave laser beam, delivered by a frequency-doubled Nd:YAG laser at 532 nm, crossed the particle beam. The scattered light from the individual particles at 532 nm was detected by a photomultiplier tube (Hamamatsu Photonics, 1P28A). The scattered signal intensity was measured by the photomultiplier, which was utilized as a measure of the relative particle size.[17] The scattered signals above a selectable threshold level triggered a pulsed KrF excimer laser at 248 nm, which was used as a light source for desorption/ionization of chemical species of particles. This LISPA-MS instrument can detect aerosols at a lower detectable limit of 0.2 μm diameter and an upper limit of 1 μm due to the transmission limit of the aerodynamic lens.[15,16] The resultant positive and negative ions were measured with a time-of-flight mass spectrometer attached with a microchannel plate detector. The ion signals from the detector were amplified, digitized, and recorded as mass spectra. Either positive- or negative-ion mass spectra were obtained by changing the voltage polarity of the instrument.

Optical Properties of Iodine-Containing Aerosols. We measured optical properties of the aerosols extinction coefficient (α_{ex}) at 532 nm by CRDS, absorption coefficient (α_{ab}) at 565 nm by PSAP (Radiance Research), and scattering coefficient (α_{sc}) at 530 nm by Nephelometer (Radiance Research, M903). The CRD spectrometer employed a probe laser (Nd^{3+}:YAG laser, Spectra Physics, LAB-130, $\lambda = 532$ nm). The CRDS reaction cell (Pyrex glass tube, 21 mm i.d.) was attached with two highly reflective plano-concave mirrors (Research Electro-Optics, 7.8 mm diameter and 1 m curvature, specified reflectivity >0.999) as described previously.[12,18–23] These mirrors were mounted 1.04 m apart. Light leaking from the end mirror was detected by a photomultiplier tube (Hamamatsu Photonics, R212UH) through band-pass filters. Synthetic air was introduced upstream of the cell, typically 3.5 slm, to keep the pressure of the cell at 1 atm. Nitrogen gas was also introduced at a flow rate of 50 sccm into the ends of the ring-down cavity, close to the mirrors, in order to minimize deterioration caused by exposure to the reactants and the products in the cell.

For CRDS, temporal decays of the signal intensity were recorded using a digital oscilloscope (PICO, ADC-212, 12-bit resolution, 50 ns/channel). In the presence of particles, the light intensity within the cavity is described by:

$$I(t) = I_0 \exp(-t/\tau) = I_0 \exp\{-(1/\tau_0 + \alpha_{ext} cd/L)t\} \quad (10)$$

where I_0 and $I(t)$ are the light intensities at time 0 and t. τ is the cavity ring-down time with aerosol samples. τ_0 is the cavity ring-down time with clean air gas and typically 75 μs. α_{ex} ($=\alpha_{sc} + \alpha_{ab}$) is the extinction coefficient of the particles inside the cavity, d the actual distance in the cavity filled with aerosols (0.9 m), L the cavity length, c the velocity of light. α_{sc} and α_{ab} stands for scattering and absorption coefficients, respectively. The CRDS spectrometer and nephelometer were calibrated using polystyrene latex particles (Duke Science Corp., 0.3 and 0.5 μm diameters). The PSAP data was corrected to 532 nm with an assumption that angstrom exponent is 1 after the correction for flow rate, spot area, and scattering coefficient based on Bond et al.[24]

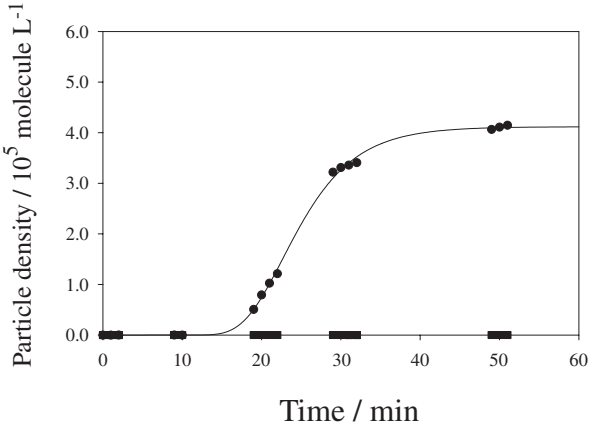

Figure 1. Temporal profiles of concentration of different particle size measured by optical particle counter. The horizontal axis shows UV-lamp irradiation time. $[CH_2I_2] = 6.4 \times 10^{12}$, $[O_3] = 1.3 \times 10^{13}$ molecule cm^{-3} in 760 Torr air diluent. ●: 0.3–0.5 μm dia., ■: >0.5 μm dia. The solid curve is for visual clarity. Particles of >0.5 μm dia. were under 100 molecule L^{-1}.

Results

Figure 1 shows the temporal profile of OPC data as a function of photoirradiation time. The initial reagent concentrations of CH_2I_2, O_2, and O_3 were 1.3×10^{13}, 6.2×10^{18}, and 2.1×10^{13} molecule cm^{-3}, respectively. Particle density in the diameter range of 0.3–0.5 μm increased up to 4×10^5 molecule L^{-1} after 40–50 min UV-irradiation, while that for particles with diameter over 0.5 μm was under 100 molecule L^{-1}. This result shows that particles below 0.5 μm diameter were dominant. With the initial concentrations of CH_2I_2, O_2, and O_3, 6.0×10^{14}, 6.2×10^{18}, and 1.1×10^{14} molecule cm^{-3}, respectively, similar temporal change was obtained.

Chemical Compositions of the Aerosols. Figure 2 shows typical positive and negative ion mass spectra of the iodine aerosols measured using LISPA-MS. The initial concentrations of CH_2I_2, O_2, and O_3 were 3.7×10^{13}, 6.2×10^{18}, and 2.1×10^{13} molecule cm^{-3}, respectively. The detected peaks in the mass spectra can be assigned to the positive and negative ions of IO_n ($n = 0$–4) and I_2O_n ($n = 0$–6) for the gas mixtures of $CH_2I_2/O_2/O_3$ in air diluent. The inset shows the detailed positive ion spectrum for IO^+ and HOI^+, which was measured under separate experiments from those for the main figure and the data were processed by the fast Fourier transform method to reduce noise levels. Positive and negative ions of I_3 and I_3O were also observed.

Figure 3 shows negative ion signals of the lower masses to charge ratios ($m/z = 20$–60), which would be derived from carbon compounds. These carbon compound signals appeared quite seldom in the observed mass spectra while those of iodine oxides appeared in almost every mass spectrum. No positive ions containing carbon species were observed. The spectra are essentially the same for both small and large particles as

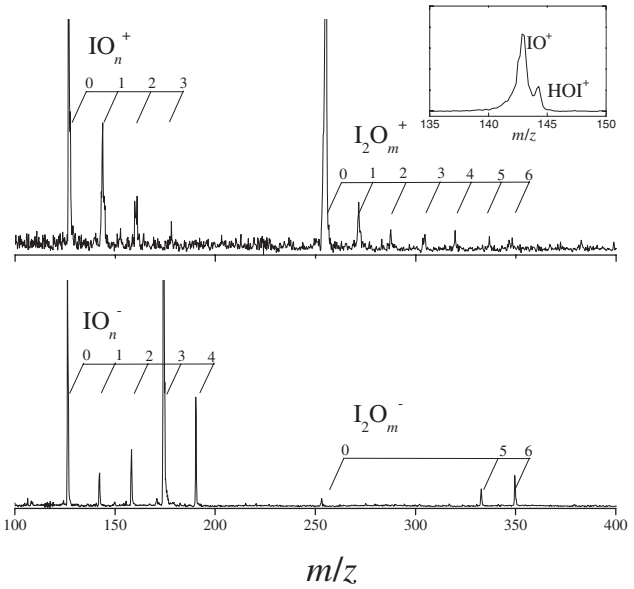

Figure 2. Positive and negative ion mass spectra of iodine-containing aerosols ($m/z = 100$–400). Experimental conditions are the same as for Figure 1. The insert shows a positive ion spectrum for $m/z = 135$–150.

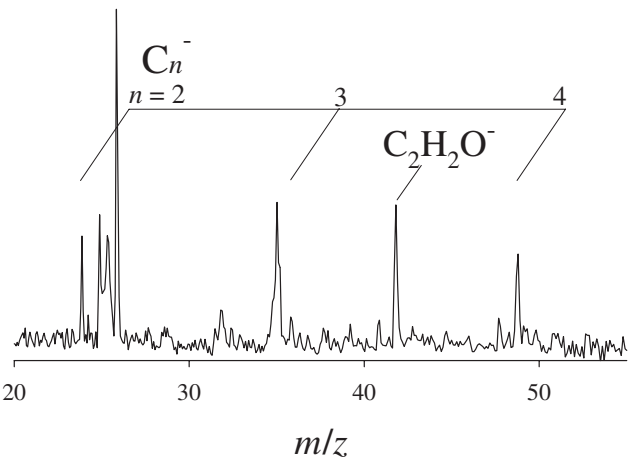

Figure 3. An example of negative ion mass spectra of iodine-containing aerosols. Experimental conditions are the same as for Figure 1.

positive and negative ions of I, I_2, and IO_n ($n = 1$–4) show no tendencies in all scattering signal intensity ranges, while the weak positive and negative ions of I_2O_n ($n = 1$–6) and I_3O_n ($n = 0$–1) appeared at larger scattering signal intensity or larger aerosol size.

Optical Properties of the Aerosols. The extinction coefficient of the iodine-containing particles was measured with CRDS while the scattering coefficient with nephelometer and the absorption coefficient with PSAP. These results are compared to each other as shown in Figure 4 with the initial concentrations of CH_2I_2, O_2, and O_3 were 6.0×10^{14}, 6.2×10^{18}, and 1.1×10^{14} molecule cm^{-3}, respectively. Using the slopes in Figure 4, single scattering albedo (SSA), which is defined as α_{sc}/α_{ex}, is calculated to be $\alpha_{sc}(\text{Neph})/\alpha_{ex}(\text{CRDS}) = 0.960 \pm 0.003$, and $1 - \{\alpha_{ab}(\text{PSAP})/\alpha_{ex}(\text{CRDS})\} = 0.959 \pm 0.007$. The SSA values obtained using two different combinations of data agree with each other within the estimated errors. We choose the SSA value of 0.96 ± 0.01 for iodine aerosols formed under our experimental conditions. Thus, the iodine aerosol has weak absorption in the visible region at least around 530 nm.

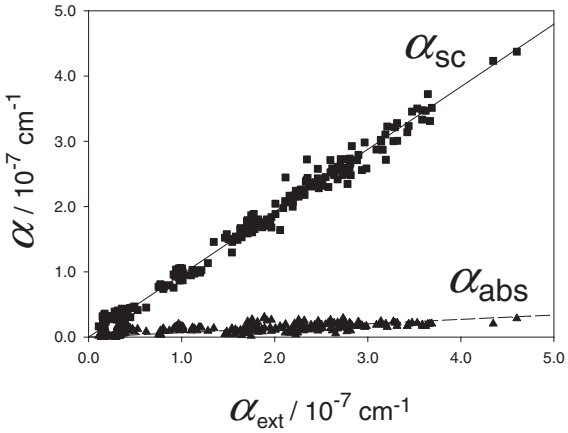

Figure 4. Comparison of extinction coefficients with scattering and absorption coefficients under dry conditions. $CH_2I_2 + O_3$ in air with UV photoirradiation. $[CH_2I_2] = 6.0 \times 10^{14}$, $[O_3] = 1.1 \times 10^{14}$ molecule cm^{-3} in 760 Torr air diluent.

Discussion

Jimenez et al.[6] investigated aerosols from the direct photolysis of CH_2I_2 in the presence of O_3 in the Caltech indoor chamber, and reported the chemical composition of iodine particles with growth time or particle size. Their experiment was performed with the concentration ranges, CH_2I_2 0.0040–1.2×10^{11} molecule cm^{-3} and O_3 0.30–1.2×10^{13} molecule cm^{-3}, lower concentration conditions than ours. With use of an Aerodyne aerosol mass spectrometer, they reported temporal and size behaviors for I^+, I_2^+, IO^+, IO_2^+, IO_5^+, I_2O^+, and $I_2O_3^+$. Based on their results they concluded that the aerosol chemical compositions did not vary with reaction time or particle size. Our results are in accord with their results, using LISPA-MS which can detect only larger particles $>0.2\,\mu$m. In our experiment, we detected ion species such as I_2O_n and I_3O_n. The chemical composition of particles are believed to contain OIO, I_2O_2, I_2O_3, I_2O_4, and I_2O_5 species as reported previously.[9–11] Carbon-containing compound ions as shown in Figure 3 indicate the contribution of carbon-containing radicals such as $CHIO_2$ and CH_2O_2 to aerosol formation. However, the results that a) the appearance probability of the carbon-containing ion signals is much lower than those of iodine-containing compound ion signals, and b) Jimenez et al.[6] did not observe the carbon-containing ion signals indicate that iodine oxides (OIO, I_2O_2, I_2O_3, I_2O_4, and I_2O_5) mainly form aerosols[9–11] and the contribution of carbon-containing radicals such as $CHIO_2$ and CH_2O_2 is small. Jimenez et al.[6] reported that the iodine particles may also include hydrogen-containing iodine species. Our experimental results for HOI^+ in the inset of Figure 3 are in accord with their report. Particle size distributions were measured previously by Jimenez et al.[6] using a scanning electrical mobility spectrometer. The reported size

distributions of iodine particles had a peak around 0.1–0.2 μm and particle growth finished within 50 min. Our results from OPC show particles of <0.5 μm diameter are dominant and particle growth almost finished within 50 min and the chemical compositions are in accord with those reported by Jimenez et al.[6] as discussed above. Thus, in our experiment, the particle size distribution is estimated to be similar to that reported by Jimenez et al.[6] Our optical measurements show that the iodine particles, with the chemical composition and size distribution as discussed above, have weak absorption in the visible region at least around 530 nm.

Conclusion

Typical marine-boundary aerosols that are produced from photochemical reactions of CH_2I_2 consist of iodine oxide species such as I_nO_m as reported by Pirjola et al.,[9] Saiz-Lopez et al.,[10] and Saunders and Plane.[11] In the present laboratory experiments with a mixture gas of CH_2I_2 and O_3 in synthetic air and UV irradiation, we found that 1) the chemical compositions and particle growth are similar to those previously reported by Jimenez et al.[6] and 2) the aerosols have weak visible absorption.

This work was supported by a Grant-in-Aid from JSPS (No. 20245005). Financial support from the Yazaki Memorial Foundation is appreciated. The authors thank Drs. A. Uchiyama and A. Yamazaki of the Meteorological Research Institute for discussion, and Yosuke Hoshino for experimental setup.

References

1 C. D. O'Dowd, M. Geever, M. K. Hill, M. H. Smith, S. G. Jennings, *Geophys. Res. Lett.* **1998**, *25*, 1661.

2 C. O'Dowd, G. McFiggans, D. J. Creasey, L. Pirjola, C. Hoell, M. H. Smith, B. J. Allan, J. M. C. Plane, D. E. Heard, J. D. Lee, M. J. Pilling, M. Kulmala, *Geophys. Res. Lett.* **1999**, *26*, 1707.

3 J. L. Grenfell, R. M. Harrison, A. G. Allen, J. P. Shi, S. A. Penkett, C. D. O'Dowd, M. H. Smith, M. K. Hill, L. Robertson, C. N. Hewitt, B. Davison, A. C. Lewis, D. J. Creasey, D. E. Heard, K. Hebestreit, B. Alicke, J. James, *J. Geophys. Res.* **1999**, *104*, 13771.

4 T. Hoffmann, C. D. O'Dowd, J. H. Seinfeld, *Geophys. Res. Lett.* **2001**, *28*, 1949.

5 C. D. O'Dowd, J. L. Jimenez, R. Bahreini, R. C. Flagan, J. H. Seinfeld, K. Hämeri, L. Pirjola, M. Kulmala, S. G. Jennings, T. Hoffmann, *Nature* **2002**, *417*, 632.

6 J. L. Jimenez, R. Bahreini, D. R. Cocker, III, H. Zhuang, V. Varutbangkul, R. C. Flagan, J. H. Seinfeld, C. D. O'Dowd, T. Hoffmann, *J. Geophys. Res.* **2003**, *108*, 4318.

7 J. B. Burkholder, J. Curtius, A. R. Ravishankara, E. R. Lovejoy, *Atmos. Chem. Phys.* **2004**, *4*, 19.

8 S. Pechtl, E. R. Lovejoy, J. B. Burkholder, R. von Glasow, *Atmos. Chem. Phys.* **2006**, *6*, 503.

9 L. Pirjola, C. D. O'Dowd, Y. J. Yoon, K. Sellegri, *Environ. Chem.* **2005**, *2*, 271.

10 A. Saiz-Lopez, J. M. C. Plane, G. McFiggans, P. I. Williams, S. M. Ball, M. Bitter, R. L. Jones, C. Hongwei, T. Hoffmann, *Atmos. Chem. Phys.* **2006**, *6*, 883.

11 R. W. Saunders, J. M. C. Plane, *Environ. Chem.* **2005**, *2*, 299.

12 S. Enami, Y. Hoshino, M. Kawasaki, *Int. J. Chem. Kinet.* **2007**, *39*, 688.

13 B. J. Finlayson-Pitts, J. N. Pitts, Jr., *Chemistry of the Upper and Lower Atmosphere*, Academic Press, San Diego, **2000**.

14 S. P. Sander, R. R. Friedl, A. R. Ravishankara, D. M. Golden, C. E. Kolb, M. J. Kurylo, R. E. Huie, V. L. Orkin, M. J. Molina, G. K. Moortgat, B. J. Finlayson-Pitts, *Chemical Kinetics and Photochemical Data for Use in Stratospheric Modeling*, Evaluation 14, Jet Propulsion Laboratory, Pasadena, CA, **2003**.

15 M. Narukawa, Y. Matsumi, J. Matsumoto, K. Takahashi, A. Yabushita, K. Sato, T. Imamura, *Anal. Sci.* **2007**, *23*, 507.

16 X. Zhang, K. A. Smith, D. R. Worsnop, J. Jimenez, J. T. Jayne, C. E. Kolb, *Aerosol Sci. Technol.* **2002**, *36*, 617.

17 M. Narukawa, Y. Matsumi, J. Matsumoto, K. Takahashi, A. Yabushita, K. Sato, T. Imamura, *Bull. Chem. Soc. Jpn.* **2008**, *81*, 120.

18 Y. Ninomiya, S. Hashimoto, M. Kawasaki, T. J. Wallington, *Int. J. Chem. Kinet.* **2000**, *32*, 125.

19 S. Enami, J. Ueda, M. Goto, Y. Nakano, S. Aloisio, S. Hashimoto, M. Kawasaki, *J. Phys. Chem. A* **2004**, *108*, 6347.

20 S. Enami, T. Yamanaka, S. Hashimoto, M. Kawasaki, K. Tonokura, *J. Phys. Chem. A* **2005**, *109*, 6066.

21 S. Enami, Y. Hoshino, Y. Ito, S. Hashimoto, M. Kawasaki, T. J. Wallington, *J. Phys. Chem. A* **2006**, *110*, 3546.

22 S. Enami, T. Yamanaka, T. Nakayama, S. Hashimoto, M. Kawasaki, D. E. Shallcross, Y. Nakano, T. Ishiwata, *J. Phys. Chem. A* **2007**, *111*, 3342.

23 S. Enami, Y. Sakamoto, T. Yamanaka, S. Hashimoto, M. Kawasaki, K. Tonokura, H. Tachikawa, *Bull. Chem. Soc. Jpn.* **2008**, *81*, 1250.

24 T. C. Bond, T. L. Anderson, D. Campbell, *Aerosol Sci. Technol.* **1999**, *30*, 582.